N. O. LASSEN AND ARNE OHRT

# MULTIPLE SCATTERING OF $\alpha$-PARTICLES

Det Kongelige Danske Videnskabernes Selskab
Matematisk-fysiske Meddelelser **36**, 9


Kommissionær: Munksgaard
København 1967

## Synopsis

The distributions in the projected angle of $\alpha$-particles having passed thin foils of Be, Al, Ni or Au, respectively, were measured. For 20 MeV $\alpha$-particles, both the shape of the distributions and the half widths were found to agree with Molière's theory. Also for 8.8 and 6.0 MeV $\alpha$-particles the half widths agree with his theory.



PRINTED IN DENMARK
BIANCO LUNOS BOGTRYKKERI A-S

## 1. Introduction

Multiple scattering of $\alpha$-particles is caused by collisions between the particles and the atomic nuclei in the stopping substance. Such collisions may result in scattering at large angles, but events of this kind are very rare, whereas each $\alpha$-particle may suffer hundreds of small deflections even in a moderately thin foil. The direction of these deflections are random, and therefore the resulting deflection does not become large and it only increases slowly with the number of collisions.

The multiple scattering was observed by RUTHERFORD in the first decade of this century[1]. Although the concept of the atomic nucleus did not exist at that time, RUTHERFORD, using a theory by LORD RAYLEIGH for the addition of randomly oriented vectors[2], correctly explained the phenomenon as being due to numerous soft collisions with the atoms. Shortly after the discovery by RUTHERFORD, the multiple scattering of $\alpha$-particles was observed by LISE MEITNER[3].

More detailed studies of the multiple scattering were performed by GEIGER (1910)[4] and by MAYER (1913)[5], both using the scintillation method and $\alpha$-particles from RaC′ and from Po, respectively. In 1932, MAURER[6], using a Geiger counter and ThC′ $\alpha$-particles, performed measurements very similar to Geiger's and compared his results with a theory by BOTHE[7]. In 1951, HUUS[8] measured the multiple scattering of protons and deuterons accelerated in a Van de Graaff. So did later BICHSEL[9], and for protons of 1–5 MeV he found very close agreement with a theory by MOLIÈRE[14] [15].

NIELS BOHR[10] took great interest in the stopping phenomena and he stressed the intimate relationship between multiple scattering and nuclear stopping. Also BETHE[11] has given several contributions to the theory of multiple scattering. The first more detailed theory, also discussing the way in which the central multiple scattering Gaussian distribution joins the distant single scattering Rutherford distribution, was given by E. J. WILLIAMS[12] [13] in 1940. In 1947, MOLIÈRE advanced his famous theory[14] [15],

and since then many other theoretical papers on this subject have appeared. The interest has, however, been mostly directed towards high energy particles, and with the above mentioned exceptions also the scanty experimental investigations have been confined to high energy particles. References may be found in a recent paper by W. SCOTT[16]. Most recently, MARION and ZIMMERMAN[17] have discussed the theories of MOLIÈRE and of NIGAM, SUNDARESAN and WU[18] and have carried out numerical calculations on the multiple scattering.

It is well known that, in the study of cosmic rays by photographic emulsions, the multiple scattering together with other stopping effects has been used as a means for determining particle properties.

## 2. Short survey of theoretical results

### A. Elementary theory

Assuming a Coulomb potential between the $\alpha$-particle and the nucleus, the scattering angle $\Theta$ in the Laboratory system for small angles is

$$\Theta = b'/p = Z_1 Z_2 e^2/pE, \tag{1}$$

where $p$ is the impact parameter, $b'$ is defined by the second equation, $Z_1$ and $Z_2$ are the charge numbers of the particle and the nucleus, respectively, $E$ is the Laboratory energy, and $e$ the electronic charge. To a first approximation the screening of the nuclear charge by the atomic electrons may be taken into account by introducing a minimum angle

$$\Theta_{\min} = b'/p_{\max} = b' Z_2^{1/3}/a, \tag{2}$$

where $a = 0.885 \cdot a_0$. Here, $a_0$ is the hydrogen Bohr radius ($5.29 \cdot 10^{-9}$ cm).

The distribution in the projected angle $x$ of a beam of $\alpha$-particles having passed a foil of thickness $t$ g cm$^{-2}$ is approximately a Gaussian with a standard deviation

$$\sigma(x) = \sqrt{\frac{\pi N_0 t}{A}} \frac{Z_1 Z_2 e^2}{E} \sqrt{\ln \frac{\Theta^*}{\Theta_{\min}}}, \tag{3}$$

where $N_0$ is Avogadro's number $6.0 \cdot 10^{23}$, $A$ is the mass number of the target nucleus, and $\Theta^*$ is a cut-off angle given by

$$\Theta^* = \sqrt{\frac{\pi N_0 t}{A}} \frac{Z_1 Z_2 e^2}{E}. \tag{4}$$

In the derivation of this result, only collisions giving deflections smaller than $\Theta^*$ are taken into account. On the average just one collision for each $\alpha$-particle has been neglected, whereas the number of collisions taken into consideration is

$$n = \Theta^{*2}/\Theta_{\min}^2, \tag{5}$$

which must be much larger than one in order that we can talk about multiple scattering.

For larger angles the projected distribution goes over in the Rutherford distribution $W(x)dx \propto x^{-3}dx$.

### B. Molière's theory

MOLIÈRE assumes a Thomas-Fermi potential. He introduces a reduced angle $\varphi$ defined by

$$\varphi = x/(\Theta^*\sqrt{B}), \tag{6}$$

where $x$ is the projected angle, $\Theta^*$ is defined by (4), and $B$ is another parameter depending on the stopping substance and the foil thickness and also slightly on the energy. We have

$$B - \ln B = \ln[\Theta^*/\Theta_a]^2 - 0.15 \tag{7}$$

where

$$\Theta_a = \frac{\hbar Z_2^{1/3}}{0.885\, a_0 m_1 v}\sqrt{1.13 + 3.76\,\alpha^2} \tag{8}$$

$$\alpha = Z_1 Z_2 e^2/(\hbar v). \tag{9}$$

Here $m_1$ and $v$ are the mass and the velocity of the $\alpha$-particle. In most cases (where $v$ is not too large or $Z_2$ not too small) $\Theta_a$ is approximately equal to $\Theta_{\min}$. As seen, $B$ is essentially a measure of the number of collisions.

The distribution in reduced angle is given by a series expansion

$$f(\varphi)d\varphi = f^{(0)}(\varphi)d\varphi + \frac{1}{B}f^{(1)}(\varphi)d\varphi + \frac{1}{B^2}f^{(2)}(\varphi)d\varphi + \ldots \tag{10}$$

where $f^{(0)}(\varphi)$ is a Gaussian

$$f^{(0)}(\varphi) = \frac{2}{\sqrt{\pi}}e^{-\varphi^2} \tag{11}$$

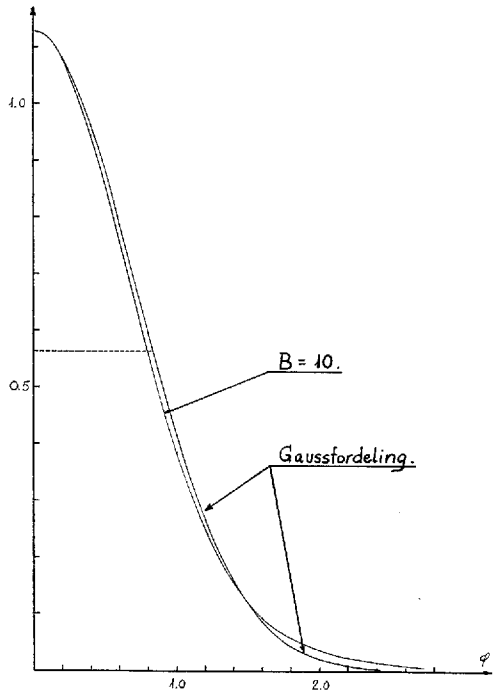


Fig. 1. The Molière distribution for a typical case ($B = 10$) and the function $f^{(0)}(\varphi)$, in the figure denoted "Gaussfordeling".

whereas $f^{(n)}(\varphi)$ are more complicated, oscillating functions. They are tabulated in refs. [15] and [16].

Fig. 1 shows the Molière distribution for a case with $B = 10$, and in the same figure the corresponding $f^{(0)}$-distribution is shown. The half width for the $f^{(0)}$-distribution is $\Delta_G = 2.35/\sqrt{2} = 1.66$. The half width $\Delta(\varphi)$ for

TABLE 1.*

| | $\Theta^* \cdot E/\sqrt{t}$ | $\Theta_a^{-1}/E$ | $\Theta^*/(\Theta_a\sqrt{t})$ |
|---|---|---|---|
| Be..... | $1.67 \cdot 10^{-2}$ | (2200) | (36.8) |
| Al..... | $3.13 \cdot 10^{-2}$ | 540 | 16.9 |
| Ni..... | $4.57 \cdot 10^{-2}$ | 197 | 9.00 |
| Au ..... | $7.05 \cdot 10^{-2}$ | 49.5 | 3.49 |

* Here, $E$ is in MeV, $t$ in mg cm$^{-2}$, $\Theta^*$ and $\Theta_a$ in radians. The table is good for Al, Ni and Au. For Be, the values are correct at 10 MeV, whereas $\Theta_a^{-1}$ and $\Theta^*/\Theta_a$ should be corrected by about + 8 % and − 13 % at 5 and 20 MeV, respectively.

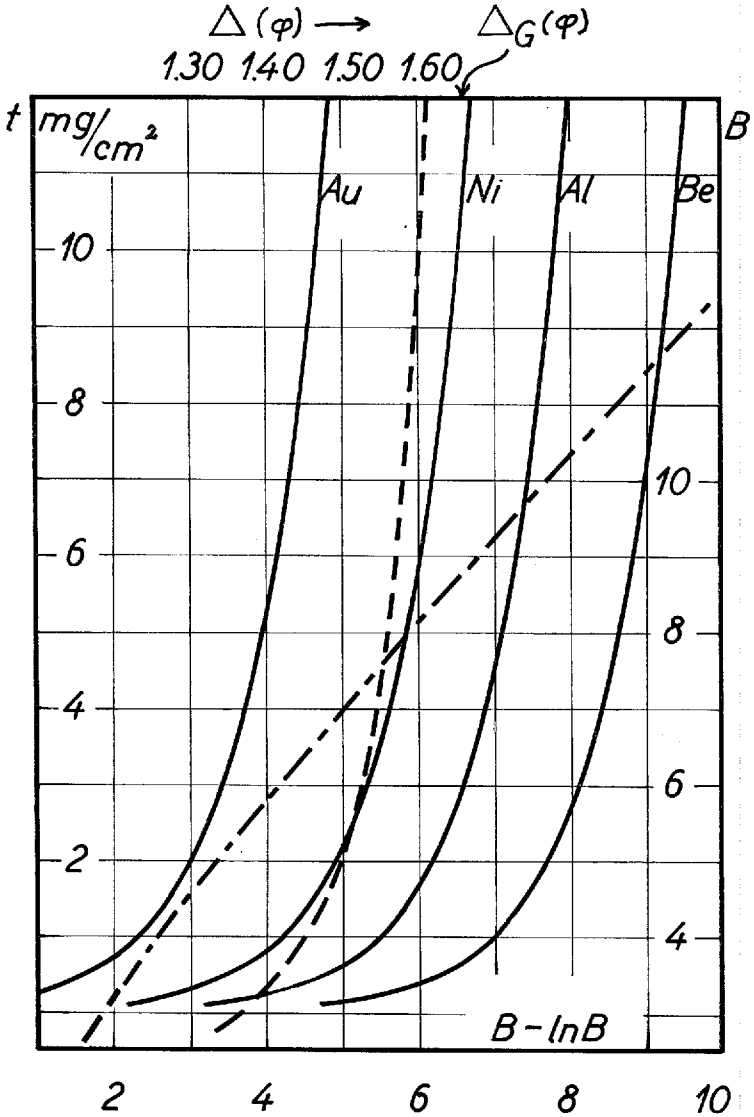


Fig. 2. $B$ and $\Delta(\varphi)$ for different foil thicknesses $t$ mg/cm² (and for $\alpha$-particles 5–20 MeV). The left-hand scale of ordinates, the full-drawn curves and the lower scale of abscissae give the relation between the foil thickness $t$ and $B - \ln B$. From the latter, $B$ may be obtained by means of the dot-and-dash curve and the right-hand scale of ordinates. Finally, the dashed line connects $B$ and $\Delta(\varphi)$ (upper scale of abscissae). The dashed curve may be slightly incorrect for the smallest $B$-values, because in formula (10) only terms until the term with $B^{-2}$ were included; anyhow, the use of the Molière theory is not well justified for the smallest $B$-values. The full-drawn curve for Be should be correct at 10 MeV, and only very slightly off at 5 and at 20 MeV.

the Molière distribution is about 5 per cent smaller. $\Delta(\varphi)$ is a function of $B$, and by drawing distributions for other $B$-values we have determined this function, which is shown in Fig. 2. This figure may also be used to find $B$ for a known foil thickness. Values of $\Theta^*$ and approximate values of $\Theta_a$ may be obtained from Table 1 (for $\alpha$-particles 5–20 MeV).

### 3. Experiments with 20 MeV $\alpha$-particles

The beam from the Copenhagen cyclotron was passed through two slits, each of width $\xi$. The second slit was placed 50 cm behind the first, and 20 cm behind the second slit a target was placed; it consisted of a pile of copper plates, each of thickness $\xi$. The plates were $10 \times 40$ mm$^2$ with the long edge, parallel to the slits, facing the beam; they were pressed hard against each other. In most experiments, $\xi = 0.45$ mm; in four cases, corresponding to the four bottom rows in Table 2, $\xi = 0.1$ mm. Foils could be placed immediately behind the second slit.

With no foil only two of the copper plates were hit by the beam, and they alone became radioactive. When a foil was inserted in the beam, however, the beam was scattered, and several plates became active. Among the produced radioisotopes only $Ga^{66}$ emits $\gamma$-quanta of energy higher than 1.5 MeV. Using a $3 \times 3$ inch NaI-crystal and discriminating against lower energy quanta, we obtained distribution curves like that shown in Fig. 3. Corrections for decay with the known half life 9.6 hours have been applied.

The figure refers to a Ni-foil 8.1 mg/cm$^2$. The curve is the Molière distribution calculated for a thickness 7.9 mg/cm$^2$. The agreement between the experimental points and the theoretical curve is as good as could be expected, both as regards the shape of the distribution and the half width. The latter is found to be $\Delta' = 6.06$ mm, in agreement with the Molière value (for 8.1 mg/cm$^2$ $\Delta_{\mathrm{Mol}} = 6.16$ mm). Correcting in the usual way for the influence of the finite slit sizes $\xi$, we obtain for the corrected half width the value $\Delta'' = ((\Delta')^2 - (1.4\,\xi)^2)^{1/2} = (6.06^2 - 0.63^2)^{1/2} = 6.03$ mm. In this case the correction is negligible, and actually the proper correction is even smaller (see next chapter). The corrections used to obtain the values $\Delta_{\mathrm{exp}}$ given in Table 2 are $-(2/3)(\Delta' - \Delta'')$, and they are, even for the thinnest foils, smaller than five per cent; in the example, $\Delta_{\mathrm{exp}} = (6.06 - 0.02)/200 = 3.02 \cdot 10^{-2}$ rad.

Fig. 4 shows a probability plot of the same distribution. The ordinates for the open points are the ratio $\sum_{i=1}^{j} n_i / \sum n_i$ in per cent (right-hand scale of

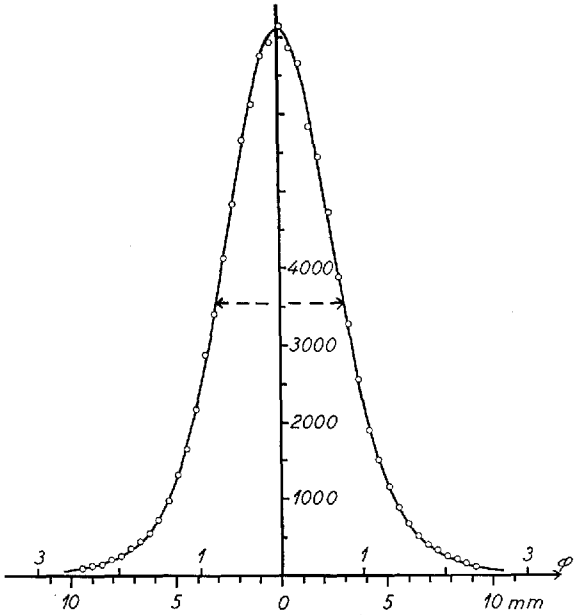


Fig. 3. Projected distribution of the beam of 20 MeV $\alpha$-particles after multiple scattering in a nickel foil, 8.1 mg/cm² thick. The points are the experimentally measured activities in counts per min. of the copper plates. The lower scale of abscissae is the distance along the target in mm; to obtain the projected angle divide by 200 mm. The upper scale of abscissae is the reduced angle $\varphi$. The full-drawn curve is the Molière distribution.

ordinates), where $n_i$ is the number of counts per min. for the $i$'th copper plate, and $\sum n_i$ is the total area below the curve in Fig. 3. The closed points are obtained after a correction for lacking measurements at large angles, i. e., when 0.0035 $\sum n_i$ is added to $\sum_{i=1}^{j} n_i$ and 0.0070 $\sum n_i$ is added to $\sum n_i$.

The Molière distribution deviates from the Gaussian $f^{(0)}(\varphi)$; the difference is only small in the central region, but quite large in the wings of the distribution. This can also be seen in Fig. 4, and it can easily be shown that the middle part of the probability plot of the Molière distribution is very nearly a straight line which corresponds to the $f^{(0)}$-function[19]. For all distributions measured with 20 MeV $\alpha$-particles we found the characteristic appearance of the probability plot shown in Fig. 4: A straight line in the middle and deviations from this line at both ends. In an attempt at expressing in a brief way the sign and the magnitude of the deviation from a Gaussian, we have adopted the following procedure. From a plot like Fig. 3, the half

width $\Delta'$ of the distribution itself was obtained; the middle part of the probability distribution gave the half width $\Delta'_G$ of the $f^{(0)}$-distribution. The fractional difference $\delta = (\Delta'_G - \Delta')/\Delta'_G$ is taken as a measure for the size of the wings and compared to the value obtained from the Molière theory. Plots like Fig. 4 were used only for illustrative purposes; a simple calculation from the values $n_i$ gives a more accurate value of $\Delta'_G$ than can be obtained

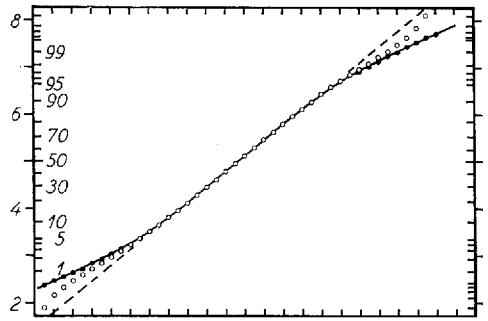


Fig. 4. The projected distribution in Fig. 3 transformed to probability paper. The ordinate is the number of "probits". A division on the axis of abscissae is 0.9 mm on the target. Open points are obtained directly from the points in Fig. 3, closed points after correction for lacking measurements at great distances from the central ray. The full-drawn curve represents the Molière distribution, the dotted line the $f^{(0)}$-function.

from a plot. For the measurements listed in Table 2, with the exception of the last four values, $\Delta'_G$ could be determined with an accuracy of about one per cent, and in most cases the same applies for $\Delta'$; only for a few of the narrower distributions the drawing of curves through the measured points was slightly more ambiguous. Thus, the absolute uncertainty of $\delta$ is about one per cent (for example: $\delta = (4 \pm 1)\ \%$ for the beryllium foils) and, as seen from Table 2, the agreement with the Molière values is good. It should here be noted that errors in $\alpha$-energy $E$, foil thickness $t$ and in any geometrical measures cancel out and do not contribute to the error in $\delta$.

From Table 2 it is also seen that the experimental half widths agree well with the Molière theory. Taking into account the uncertainty of $\Delta_{exp}$, which is estimated to about 4 per cent, the only deviations from the Molière theory which may (or may not) be significant appear in the results for aluminium foils of 1.8 and 3.1 mg/cm². It is interesting to note that BICHSEL (9) for 1–5 MeV protons also found excellent agreement with the Molière theory, just with the exception of thin aluminium foils.

For the thin Ni-foils, 0.1–0.9 mg/cm², the geometry was changed, the slit widths being reduced to 0.1 mm. The activities obtained were much

TABLE 2. Multiple Scattering of 20 MeV α-particles.*

| Substance | $t$ mg/cm² | $E$ MeV | $B$ | $\Theta^*$ $10^{-3}$rad | $\Theta^*/\Theta_a$ | $\Delta_{ET}$ $10^{-2}$rad | $\Delta_{Mol}$ $10^{-2}$rad | $\Delta_{exp}$ $10^{-2}$rad | $\delta_{Mol}$ % | $\delta_{exp}$ % |
|---|---|---|---|---|---|---|---|---|---|---|
| Be..... | 5,0 | 19,4 | 11,1 | 1,92 | 70 | 0,92 | 1,01 | 0,97 | 4 | 4 |
| „ ..... | 10,0 | 18,6 | 11,9 | 2,84 | 100 | 1,43 | 1,56 | 1,49 | 4 | 4 |
| Al..... | 1,8 | 19,8 | 8,2 | 2,11 | 23 | 0,87 | 0,94 | 0,80 | 6 | 6 |
| „ ..... | 3,1 | 19,6 | 8,8 | 2,82 | 30 | 1,22 | 1,31 | 1,39 | 5 | 5 |
| „ ..... | 5,8 | 19,3 | 9,5 | 3,90 | 41 | 1,76 | 1,88 | 1,84 | 5 | 5 |
| „ ..... | 7,1 | 19,2 | 9,8 | 4,34 | 45 | 1,99 | 2,15 | 2,16 | 5 | 4 |
| „ ..... | 10,2 | 18,8 | 10,1 | 5,32 | 54 | 2,50 | 2,68 | 2,64 | 5 | 5 |
| Ni..... | 1,8 | 19,8 | 6,7 | 3,10 | 12 | 1,15 | 1,23 | 1,20 | 7 | 7 |
| „ ..... | 3,6 | 19,7 | 7,5 | 4,40 | 17 | 1,74 | 1,87 | 1,87 | 6 | 5 |
| „ ..... | 6,3 | 19,4 | 8,1 | 5,90 | 23 | 2,44 | 2,62 | 2,57 | 6 | 6 |
| „ ..... | 8,1 | 19,3 | 8,4 | 6,76 | 26 | 2,86 | 3,08 | 3,02 | 5 | 5 |
| „ ..... | 10,8 | 19,1 | 8,8 | 7,88 | 30 | 3,40 | 3,66 | 3,59 | 5 | 5 |
| Ni..... | 0,1 | 20 | 3,0 | 0,72 | 3 | 0,17 | 0,18 | 0,21 | 17 | 14 |
| „ ..... | 0,22 | 20 | 4,1 | 1,07 | 4 | 0,30 | 0,32 | 0,35 | 12 | 8 |
| „ ..... | 0,45 | 20 | 5,0 | 1,53 | 6 | 0,48 | 0,51 | 0,51 | 10 | 12 |
| „ ..... | 0,90 | 19,9 | 5,8 | 2,17 | 8,5 | 0,74 | 0,80 | 0,79 | 8 | 14 |

* The first column in this table gives the stopping substance, column 2 the foil thickness and column 3 the mean energy of the α-particles inside the foil. The next three columns give parameters from the Molière theory. $\Delta_{ET}$ is the half width calculated from the elementary theory, i. e., using formula (3) in which, however, $\Theta_{min}$ has been replaced by $\Theta_a$, $\Theta^*/\Theta_a$ being taken from Table 1. $\Delta_{Mol} = \Delta(\varphi)\Theta^*\sqrt{B}$ is obtained by means of Table 1 and Fig. 2. As for $\delta$, see text.

smaller and hence the uncertainties larger, in $\Delta_{exp} \sim 10$ per cent and in $\delta_{exp} \sim 4$ per cent. At least for the two thinnest foils the number of collisions made by the α-particles is quite small and one can hardly talk about multiple scattering; therefore, the theories do not apply. Nevertheless, the calculated and the measured half widths agree fairly well.

Fig. 5 shows the result for nickel foils of various thickness; it may be noted that the half width $\Delta$ increases roughly, but not exactly, proportional to the square root of the foil thickness $t$.

## 4. Experiments with ThC + C' α-particles

A source of ThB and its daughters was prepared in the usual way. A piece of a platinum wire with a one mm sphere at one end was placed in a small chamber containing thoron, emanating from radiothorium. This source emits α-particles of energies 8.8 and 6.0 MeV, which were detected

by a silicon solid-state detector. During the measurements a slit was placed close to the source, a second slit which could be covered by a foil was placed 10 cm away, and a third slit 20 cm from the first slit. All three slits were placed parallel, and each was 0.52 mm in width. The third slit and the counter behind it could be moved sideways by means of a micrometer screw, and for each setting the $\alpha$-spectrum was recorded on a 100 channel

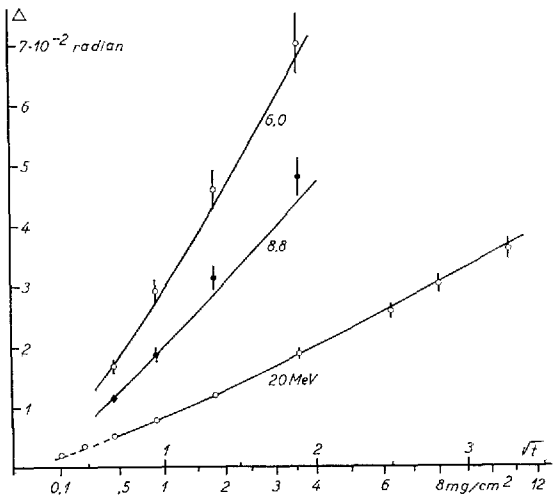


Fig. 5. The half width $\Delta$ of the projected distribution after multiple scattering in nickel foils of various thickness $t$ mg/cm² for $\alpha$-particles with incoming energies 6.0, 8.8, and 20 MeV. The points are experimental values, the curves are calculated from Molière's theory.

pulse height analyzer. From the spectra the angular distribution of the 8.8 and 6.0 MeV $\alpha$-particles, respectively, could be obtained. Fig. 6 shows an example.

In these experiments the geometry was not as good as in the experiments reported in the preceding paragraph, and it is essential to correct the measured half widths for the influence of the finite slit widths. With no foil the distribution is a curve composed of parabolic arcs[19]; this curve and corresponding experimental measurements are shown in Fig. 7, and it should be noted, that the distribution deviates from a Gaussian in a way opposite to the Molière distribution. Therefore, and since the geometrical corrections are not negligible, we cannot measure the shape of the distribution sufficiently accurate for a close comparison with the Molière distribution, and we cannot determine the quantity $\delta$.

Naturally, by lengthy calculations it would be possible to find for any foil

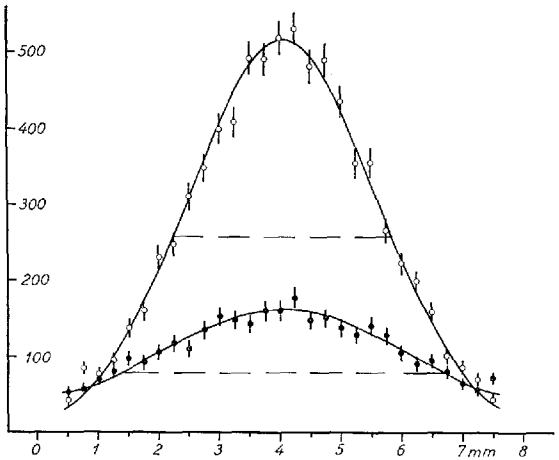


Fig. 6. Projected distribution after multiple scattering in an aluminum foil, 4.0 mg/cm² in thickness, for α-particles with incoming energies 8.8 and 6.0 MeV (open and closed points, respectively). The ordinate is the number of α-particles per 30 min., the abscissa is the displacement of the third slit and the counter. To obtain the projected angle divide by 94 mm, the distance from the foil to the counter slit. All slit widths are 0.52 mm. The curves are Gaussians with half widths, 3.6 and 5.3 mm, respectively.

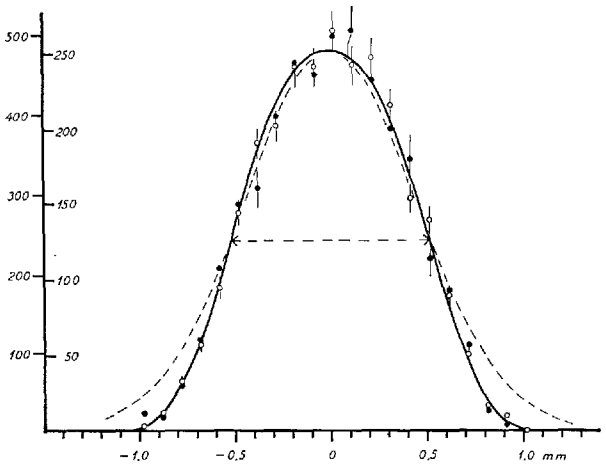


Fig. 7. Projected distribution without foil. Open points refer to 8.8 MeV α-particles (left-hand scale of ordinates), closed points to 6.0 MeV α-particles (right-hand scale of ordinates). The full-drawn curve is the expected distribution (see text). For comparison, the dotted line shows a Gaussian with the same half width.

TABLE 3. Multiple Scattering of ThC + C' $\alpha$-particles.*

| Substance | $t$ mg/cm² | $E$ MeV | $B$ | $\Theta^*$ $10^{-3}$rad | $\Theta^*/\Theta_a$ | $\Delta_{ET}$ $10^{-2}$rad | $\Delta_{Mol}$ $10^{-2}$rad | $\Delta_{exp}$ $10^{-2}$rad |
|---|---|---|---|---|---|---|---|---|
| Be..... | 5,0 | 7,46 | 11,1 | 5,00 | 70 | 2,42 | 2,65 | 2,45 |
| Al..... | 1,8 | 8,41 | 8,2 | 4,97 | 23 | 2,06 | 2,23 | 2,18 |
| „ ..... | „ | 5,54 | 8,2 | 7,55 | 23 | 3,14 | 3,38 | 3,29 |
| „ ..... | 4,0 | 7,87 | 9,1 | 7,96 | 34 | 3,52 | 3,76 | 3,68 |
| „ ..... | „ | 4,80 | 9,1 | 13,0 | 34 | 5,73 | 6,18 | 5,6 |
| Ni..... | 0,45 | 8,71 | 5,0 | 3,51 | 6 | 1,11 | 1,18 | 1,14 |
| „ ..... | „ | 5,96 | 5,0 | 5,14 | 6 | 1,62 | 1,72 | 1,67 |
| „ ..... | 0,9 | 8,63 | 5,9 | 5,03 | 8,5 | 1,73 | 1,87 | 1,87 |
| „ ..... | „ | 5,87 | 5,9 | 7,39 | 8,5 | 2,54 | 2,74 | 2,92 |
| „ ..... | 1,8 | 8,49 | 6,7 | 7,20 | 12 | 2,67 | 2,88 | 3,13 |
| „ ..... | „ | 5,68 | 6,7 | 10,8 | 12 | 4,04 | 4,32 | 4,6 |
| „ ..... | 3,6 | 8,18 | 7,5 | 10,6 | 17 | 4,20 | 4,40 | 4,8 |
| „ ..... | „ | 5,28 | 7,5 | 16,4 | 17 | 6,50 | 6,82 | 7,0 |
| Au..... | 0,39 | 8,75 | 2,2 | 5,03 | 2,2 | 1,05 | (0,9) | 0,8 |
| „ ..... | „ | 6,02 | 2,2 | 7,32 | 2,2 | 1,53 | (1.3) | 1,51 |
| „ ..... | 0,45 | 8,74 | 2,4 | 5,40 | 2,3 | 1,17 | (1.1) | 1,36 |
| „ ..... | „ | 6,01 | 2,4 | 7,86 | 2,3 | 1,70 | (1,5) | 1,86 |
| „ ..... | 0,54 | 8,74 | 2,8 | 5,92 | 2,6 | 1,35 | 1,30 | 1,37 |
| „ ..... | „ | 6,00 | 2,8 | 8,64 | 2,6 | 1,97 | 1,94 | 1,93 |
| „ ..... | 0,70 | 8,72 | 3,1 | 6,76 | 2,9 | 1,64 | 1,65 | 1,69 |
| „ ..... | „ | 5,99 | 3,1 | 9,83 | 2,9 | 2,39 | 2,40 | 2,40 |
| „ ..... | 0,92 | 8,71 | 3,5 | 7,76 | 3,4 | 2,00 | 2,08 | 2,27 |
| „ ..... | „ | 5,97 | 3,5 | 11,3 | 3,4 | 2,92 | 3,02 | 3,17 |
| „ ..... | 1,07 | 8,69 | 3,7 | 8,39 | 3,6 | 2,24 | 2,33 | 2,23 |
| „ ..... | „ | 5,95 | 3,7 | 11,2 | 3,6 | 3,25 | 3,38 | 3,40 |
| „ ..... | 1,31 | 8,68 | 4,0 | 9,30 | 4,0 | 2,56 | 2,71 | 2,68 |
| „ ..... | „ | 5,93 | 4,0 | 13,6 | 4,0 | 3,77 | 3,96 | 3,84 |

* For further explanation, see Table 2.

the distribution to be expected according to Molière's theory. In view of the rather limited number of counts, of course especially in the wings of the distributions, such calculations would hardly be reasonable. We have used the GIER electronic computer of the Niels Bohr Institute to calculate the total half width to be expected if the multiple scattering distribution were a Gaussian with standard deviation $\sigma$; the result is shown in Fig. 8. It is found that the proper correction to apply to the measured half width is smaller than would correspond to a quadratic addition of the multiple scattering half width and the "zero-thickness" half width; this is the justification for the correction used in the preceding paragraph.

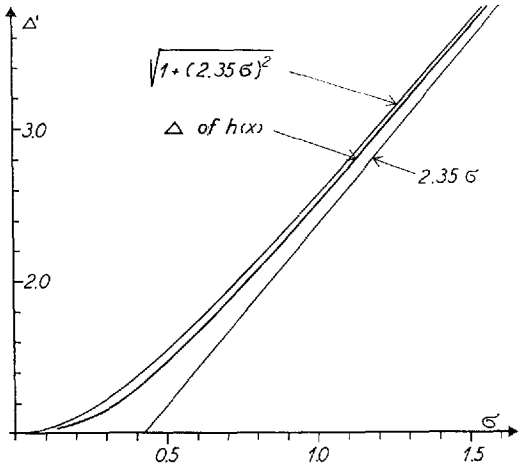


Fig. 8. Correction of the measured half width due to finite slit widths. The ordinate is the measured half width, the abscissa the standard deviation of the (here assumed) Gaussian distribution of the multiple scattering. The lower curve with zero correction. The upper curve is obtained by quadratic addition of half widths. The middle curve gives the half width of the distribution curve $h(x)$ to be expected with the above mentioned assumption (and as found by numerical calculations). The unit for abscissae and ordinates is $2\,\xi$, where $\xi$ is the common width for the three slits.

The results obtained for Th $\alpha$-particles are summarized in Table 3. The uncertainty in $\Delta_{exp}$ is estimated to about 7 per cent, perhaps slightly higher for the broadest distributions, where the lack of good statistics is most pronounced. No significant departures from the Molière theory are observed.

The beryllium, aluminum and nickel foils were obtained commercially. The gold foils were made by evaporation *in vacuo* onto a glass plate covered by a thin layer of sugar, and afterwards they were floated off in water. Their thickness was determined from the energy loss by the $\alpha$-particles, a 512 channel pulse-height analyzer being used to record the $\alpha$-spectra. Of course, the foils are thinner than corresponding to the limit of validity of the Molière theory; nevertheless, the theory gives results closely agreeing with the experimental values.

These experiments were carried out at the Niels Bohr Institute, The University of Copenhagen. For valuable help our thanks are due Mr. N. O. Roy Poulsen, mag. sc., and the cyclotron group.

## References


1. E. Rutherford: Phil. Mag. **12**, 143, 1906.
2. Lord Rayleigh: Theory of Sound, 2. Ed. 1894, p. 39.
3. Lise Meitner: Phys. Zeitschr. 8, 489, 1907.
4. H. Geiger: Proc. Roy. Soc. A **83**, 492, 1910.
5. F. Mayer: Ann. d. Phys. **41**, 931, 1913.
6. G. Maurer: Zs. f. Phys. **78**, 395, 1932.
7. W. Bothe: Zs. f. Phys. **4**, 161 und 300, 1921.
8. T. Huus: Mat. Fys. Medd. Dan. Vid. Selsk. **26**, no. 4, 1951.
9. H. Bichsel: Phys. Rev. **112**, 182, 1958.
10. N. Bohr: Mat. Fys. Medd. Dan. Vid. Selsk. **18**, no. 8, 1948.
11. H. A. Bethe: Phys. Rev. **70**, 821, 1946.
12. E. J. Williams: Phys. Rev. **58**, 292, 1940.
13. E. J. Williams: Revs. Mod. Phys. **17**, 217, 1945.
14. G. Molière: Zs. f. Naturf. **2a**, 183, 1947.
15. G. Molière: Zs. f. Naturf. **3a**, 78, 1947.
16. W. J. Scott: Revs. Mod. Phys. **35**, 231, 1963.
17. J. B. Marion and Barbara A. Zimmerman: The Lemon Aid Preprint Series in Nuclear Physics, October 1966.
18. B. P. Nigam, M. K. Sundaresan and T.-Y. Wu: Phys. Rev. **115**, 491, 1959.
19. N. O. Lassen og Arne Ohrt: Fysisk Tidsskrift **65**, 65, 1967.


Indleveret til Selskabet den 1. september 1967.
Færdig fra trykkeriet den 31. december 1967.